IEEE Access
Multidisciplinary ⋮ Rapid Review ⋮ Open Access Journal

Received September 15, 2021, accepted October 3, 2021, date of publication October 6, 2021, date of current version October 18, 2021.

Digital Object Identifier 10.1109/ACCESS.2021.3118539

Control Efficient Power Allocation of Uplink NOMA in UAV-Aided Vehicular Platooning

YANGLONG SUN, (Graduate Student Member, IEEE), KE ZHENG, AND YULIANG TANG, (Member, IEEE)

Department of Information and Communication Engineering, Xiamen University, Xiamen 361005, China

Corresponding author: Yuliang Tang (tyl@xmu.edu.cn)

This work was supported by the National Natural Science Foundation of China under Grant 61731012, Grant 61801409, and Grant 91638204.

ABSTRACT Power allocation in non-orthogonal multiple access (NOMA) systems is essential to avoid multi-user detection failure. However, controlling the uplink transmission power brings extra signaling overhead, especially in dynamic environments. In this paper, we investigate the uplink transmission power allocation problem in an unmanned aerial vehicle (UAV)-aided platooning NOMA system, where the UAV acts as a relay to assist inter-vehicle communications. Platoon vehicles are admitted to the same vehicle-to-UAV channel via our proposed sequence-based power allocation (SPA) strategy. Instead of achieving the optimal energy efficiency, our goal is to design a simple yet effective power control scheme. Specially, in SPA strategy, vehicles determine their transmission power according to their positions in the platoon. Considering platoon dynamics due to vehicle mobility, a power-reserved mechanism is further incorporated in the proposed strategy to pre-allocate power resources for newly joined vehicles. In addition, a power-moving mechanism is further employed to guarantee the uplink signal-to-interference-plus-noise ratio (SINR) of vehicles by changing vehicle transmission power into higher levels during vehicle leaving a platoon. As the system only needs to update vehicle positions for the SPA strategy, only a small amount of signaling is required in our power allocation strategy. Extensive simulation results are provided to demonstrate that the proposed SPA strategy ensures the required SINR of platoon communication in different dynamic scenarios.

INDEX TERMS UAV relay, vehicle platooning, non-orthogonal multiple access, power allocation.

I. INTRODUCTION

Non-orthogonal multiple access (NOMA) is a promising technology to improve spectrum efficiency by allowing users to share the time/frequency resources [1]. For instance, the grant-free (GF) users can access to the channel occupied by the grant-based (GB) users [2]. Therefore, power allocation in NOMA is essential to control interference among users and satisfy quality of service (QoS) requirement [3], [4]. Existing research works have studied how to optimize the power allocation in conventional NOMA systems, which may incur extra signaling overhead and channel access latency [5]. To address this issue, several research works have been devoted to simplify power allocation schemes. For example, without requiring the centralized control of the base station (BS), users can adopt a channel inversion power control policy to determine their transmission powers [6]. Another way is to control the access contention when user transmission powers are fixed, where users decide whether to join a channel according to the transmission determination criterion broadcasted by the BS [2]. Specially, a number of emerging methods, such as evolutionary game, user pairing, and reinforcement learning, were invoked to determine optimal system decisions [7]–[9].

NOMA is also considered in vehicular networks to address the challenges of massive connectivity [10]–[12]. For instance, in a network system that amalgamates NOMA with spatial modulation, the throughput of high priority flows is maximized while the QoS of low priority flows is supported [10]. Besides achieving optimal power allocation with various objectives, some power control schemes with low system overhead, such as the clustering-based, the machine learning-based, have been studied [13], [14]. In addition, a cache-aided NOMA is proposed to treat the

The associate editor coordinating the review of this manuscript and approving it for publication was Barbara Masini.

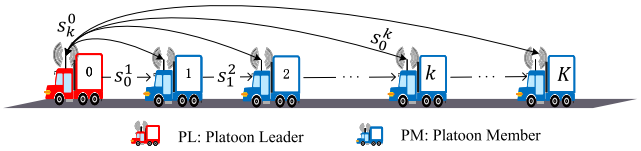

FIGURE 1. A scenario of vehicle platoon communication.

pre-cached contents of vehicles as decoded signals to get high throughput [15]. However, few literature works focus on the safety-related message transmission with NOMA-aided vehicular communication, which requires a low-latency transmission power management [10]. This paper applies the power-domain NOMA in the vehicle platooning, which is an important application in 5G networks [16], [17]. Fig. 1 illustrates the messages transmitted among platoon vehicles, where vehicle 0 is a platoon leader (PL) and the other vehicles are platoon members (PMs). s_0^k is the message from PL to vehicle k ($\forall\ 1 \leq k \leq K$), by which the PL informs the PMs of the desired speed, distance headway, and some road conditions. For two adjacent vehicles k and $|k+1|$ in the platoon, the front vehicle k sends message s_k^{k+1} to vehicle $|k+1|$ to share real-time speed, acceleration, and position information. The message s_k^0 is from PM to PL, which contains the vehicle joining/leaving request and message acknowledgment.

Utilizing NOMA in platoon brings two advantages as compared to traditional orthogonal multiple access (OMA) technoligies. One is reducing the platoon's occupation of radio resources, as NOMA has a higher spectral efficiency than OMA. Another is shortening the cycle delay. As shown in Table 1, with a single channel, the spent time of all vehicles completing a message exchange (referred to as *cycle delay*) via the OMA technology is $(2K+1)$ slots (the time period of one message sending). Consider message s_k^{k+1} have both different source nodes and destination nodes, and s_0^k is usually a broadcast message, we can only apply NOMA technology on transmitting message s_k^0. The PMs send messages in the same slot and the PL decodes the superimposed signal via successive interference cancellation (SIC) and parallel interference cancellation (PIC) receivers. The cycle delay of "NOMA/OMA" is $(K+2)$, which is less than "OMA" with the condition of $K > 1$.

However, the above "NOMA/OMA" faces challenges in utilizing NOMA, as the transmission power of PMs needs to be carefully controlled to ensure the reliability of transmission, which brings a severe system signaling overhead. What's more, the channel of vehicle-to-vehicle is complicated due to the possible obstacles [18]. To solve this issue, we first make the whole platoon as one group to obtain a stable group member. Then, using an unmanned aerial vehicle (UAV) as a relay in intra-platoon communication, we reduce the channel dynamics [19], [20], as illustrated in Fig. 2. All messages are firstly sent from platoon vehicles to UAV (P2U), then the UAV sends back the messages to platoon vehicles. For instance, PM vehicle k sends message s_k^0 to the UAV with the messages of other vehicles via NOMA, then the UAV decodes the superimposed signal and re-superimposes the signals by power allocation, as shown in Fig. 2(a). At last, the UAV sends the new superimposed signal to the platoon vehicles (U2P), by which the PL gets the messages from vehicle k, see Fig. 2(b). The UAV in our system not only can make NOMA implementation in platoon more practical but also can shorten the cycle delay. As shown in Table 1, by using NOMA in the transmissions of P2U and U2P, the time cost is only 2 slots. Assuming the receivers in UAVs and vehicles work in perfect SIC, the proposed UAV-NOMA technology brings considerable benefits to vehicle platoon communication. For the power control issues, we propose a sequence-based power allocation (SPA) strategy, where the vehicles set the power according to their positions in the platoon. The UAV generates a power matrix according to the different platoon sizes

TABLE 1. Delay comparison of different communication scheme (①: Messages transmitted via OMA; ②: Messages transmitted via NOMA; ③: Messages transmited from platoon vehicles to UAV; ④: Messages transmitted from UAV to platoon vehicles).

OMA		NOMA/OMA		UAV-NOMA	
Message	Slot	Message	Slot	Message	Slot
s_0^k	1	s_0^k	1	③ s_0^k, s_k^{k+1}, s_k^0	1
s_k^{k+1}	K	① s_k^{k+1}	K	④ s_0^k, s_k^{k+1}, s_k^0	1
s_k^0	K	② s_k^0	1		
Cycle Delay	$2K+1$	Cycle Delay	$K+2$	Cycle Delay	2

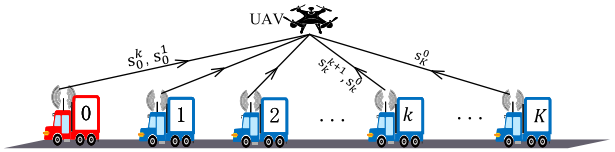

(a) Signals from platoon vehicles to UAV

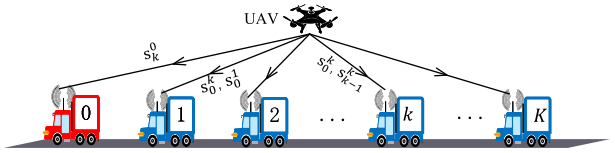

(b) Signals from UAV to platoon vehicles

FIGURE 2. The scenario of UAV-aided vehicle platoon communication.

(the number of vehicles in a platoon) and updates the platoon states in real-time. Therefore, given a platoon, the system has a unique power allocation result, and the vehicle transmits messages on the sequence-related power without an extra handshaking process.

In this paper, we aim to design a power allocation strategy with a low-signaling overhead. For a stable platoon whose distance headway and the members are fixed, the vehicles keep their power unchanged and transmit in the GF manner. However, the events of vehicle joining and leaving are inevitable in the platoon, which produces a dynamic platoon and affects the power allocation results. Especially, the scenario of vehicle joining is equivalent to the GF users admitted into the channel of the GB users [2]. To provide a GF transmission and reduce the interference, a power-reserved mechanism is invoked, in which the joining vehicle is pre-considered in the SPA strategy. A vehicle left the platoon stops transmitting messages on the current channel, which has no negative influence on the signal-to-interference-plus-noise ratio (SINR) of the other PMs. However, the channel status is changing with the platoon closing the extra distance headway caused by vehicles leaving and the vehicles need to change their power to maintain the desired SINR [9]. To decrease the overhead of power changing, the vehicles suffering SINR dropping switch their power values to other levels based on our power-moving mechanism.

The main contributions of this paper are summarized as follows:

1) We investigate the vehicle safety message transmission problem and then propose an SPA strategy to simplify the procedure of power allocation with a low signaling overhead;
2) We theoretically analyze the effect of the platoon dynamics, including vehicle joining and vehicle leaving, on the SINR of the vehicles, which can be beneficial to proposing power adjustment mechanism;
3) We employ a power-reserved mechanism for newly joining vehicles in the platoon, by which the newly joining vehicles can transmit messages to the UAV on a power level that does not affect the transmission of other vehicles;
4) We develop a power-moving mechanism to ensure the SINR when the platoon declines the distance headway gap caused by vehicles leaving.

The remainder of this paper is organized as follows: Section II summarizes the existing work about the NOMA and platooning. In Section III, we present the system model. The proposed SPA strategy and its performance analysis are presented in Section IV. Section V discusses the influences on SINRs from the dynamic changes of the platoon. In Section VI, we introduce our power allocation algorithm and propose two mechanisms for platoon changing. Section VII provides the simulation results and the conclusion is made in Section VIII.

II. RELATED WORK

Vehicle platoon can effectively solve the safety problems, reduce fuel emissions, and improve traffic efficiency [17]. The stability and safety of the platoon are improved significantly by sharing the basic safety messages and cooperative awareness messages among vehicles [21]. Communications in a platoon include: (1) downlink, the PL broadcasts periodic information such as running speed, acceleration, position, brake, and communication resource allocation decisions to the PMs; and (2) uplink, PMs send beacon messages (such as confirmation message, position, and speed) and randomly generated requests (i.e., joining or leaving a platoon) to the PL [12], [16]. The message transmission requires high reliability and low latency to prevent vehicle collision, especially when the inner-platoon space is small and the vehicle velocity is high [22].

The emerging vehicle-to-infrastructure (V2I) technologies, such as vehicle-to-base station (V2B) and vehicle-to-roadside unit (V2R), enhance inter-vehicle communication via providing new radio access and extra communication links [23], [24]. However, the infrastructures are not always available because of the coverage holes [25]. Applying UAVs in vehicular networks, researchers achieve an on-demand communication support system, where the UAV acts as a flying BS [19], [26]. Considering UAVs are of importance in sensing a wide range road area, we logically bring the UAV to our platoon communication. In a C-V2X (cellular vehicle-to-everything) network system, the number of vehicles communicating simultaneously can be improved significantly via subchannel size selection and resource block pairs allocation [24]. However, the scarcity of radio resources is still challenging, as the platoon needs to occupy more resource blocks for the non-congestion and high-rate communication [14], [16].

Due to easy compatibility with existing networks and high spectrum efficiency, the power-domain multiplexing NOMA technology is studied widely in the literature [27], [28]. The power allocation determines the QoS, especially in the uplink scenario [4]. Thus, because no centralized control, the GF protocols may fail in multi-user detection if the number of active users is large [29], [30]. A concept of semi-grant-free (SGF) transmission has been proposed, in which the GF users share spectrum resources with GB users in an SGF NOMA network [2], [31]. In this paper, we also aim to design a transmission mechanism based on the SGF protocol.

However, the power allocation in uplink NOMA is still tricky. If one user changes power, the SINR of the user and the others would be changed. To solve the problem, adjusting the power of every node simultaneously is a potential way. For instance, with the constraints of power consumption and delay, the power adjusting process is formulated into a multivariate nonlinear optimization problem which is solved by an iterative particle swarm optimization algorithm [3]. Similarly, to maximize the system throughput, a suboptimal fractional transmission power control-based decay factor is utilized to calculate the power of every user, where the user with a

lower channel gain occupies more power with the decay factor increased. To decrease the computational complexity, the decay factor is optimized via computer simulations a priori and remains fixed during the transmission time [32]. Some online algorithms based on monotonic optimization theory and matching theory are efficient in finding an optimal power allocation decision [33], [34].

Energy efficiency and outage probability are the factors that need to be explored in power allocation. Generally, the user which is first decoded needs a higher power. In terms of the circuit energy consumption of devices, the NOMA-based wireless-powered communication network (WPCN) consumes more energy than OMA-based WPCN [35]. By optimizing subchannel assignment and power allocation, the energy efficiency of the downlink NOMA network shows better improvement than orthogonal frequency division multiple [34]. Similarly, with minimum rate requirements, a tradeoff between spectrum efficiency and energy efficiency is achieved by solving a multi-objective optimization problem in a hybrid network of NOMA and OMA [36]. What's more, the energy efficiency is affected directly by the total power of the system and the number of nodes on one channel, which means the capacity should be carefully designed [37]. The capacity also affects the system outage probability significantly. For instance, the outage probability performance goes down exponentially as the number of users increases [38]. Fortunately, by setting an appropriate SINR and controlling the number of users, a suitable outage probability can be obtained. Thus, in this paper, we focus on the SINR controlling instead of exploring the system outage probability directly.

III. SYSTEM MODEL

In this section, we present the network model, the platoon model, and the communication model, respectively.

A. NETWORK MODEL

We design a UAV-aided platooning communication system under the C-V2X architecture. Vehicles in the platoon and the UAV are equipped with a single transceiver antenna and exchange messages with each other via the "PC5" interface [23]. The BS assigns resource blocks to the UAV and vehicles within the cell radio coverage, otherwise, a carrier sensing mechanism is utilized to avoid transmission collision [39]. The Global Positioning System provides location and time-synchronization service in our solution.

The platoon adopts a UAV to enhance the inter-platooning communication as needed. For instance, when the BS is overloaded by serving several platoons, or the platoon suffers from high contention for requesting radio resources. We do not consider the scenarios, like tunnels and streets with high buildings, which are unsuitable for UAV flying. The head vehicle V_0 is always as the PL, and every vehicle can carry and charge for the UAV. Considering the limited battery life of UAV, one platoon carries several UAVs and only one of them is active at a time. Due to space limitations, we only apply NOMA in the phase of P2U link, while a broadcast manner is considered in the phase of U2P link.

B. PLATOON MODEL

We consider a platoon $\boldsymbol{V}_0^K = \{0, 1, \cdots, K\}$, as shown in Fig. 2. The platoon size is $\left|\boldsymbol{V}_0^K\right| = K+1$. A vehicle with a sequence number of k is denoted by $V_k \in \boldsymbol{V}_0^K, \forall\, 0 \le k \le K$. A sub-platoon is defined as $\boldsymbol{V}_i^j = \{i, i+1, \cdots j\}$, where $0 \le i, j \le K$, $i \le j$, and $\boldsymbol{V}_i^j \subseteq \boldsymbol{V}_0^K$; $\boldsymbol{V}_i^j = \varnothing$ when $i > j$, which means the sub-platoon contains no vehicle. In a two-dimensional coordinate system, we set the coordinates of the UAV and V_k as (x^u, H) and $\left(x_k^v, 0\right)$, respectively, where $H \ge 0$ indicates the UAV height (ignore the height of the antenna and the vehicle), $x^u, x_k^v \ge 0$. The platoon has only one distance headway d (larger than the body length of vehicles), which means the vehicles are even distributed. Thus, we have $x_k^v = x_0^v + k \cdot d$. The distance between UAV and V_k is

$$L_k = \sqrt{H^2 + (x_k)^2} \tag{1}$$

where $x_k = \left|x^u - x_k^v\right|$ indicates the horizontal distance between the UAV and V_k. For a stable platoon, the distance headway is fixed to d, thus a vehicle calculates its sequence numbers by $V_k = \left[\frac{x_k^v - x_0^v}{d}\right]$ where $[\cdot]$ means rounding.

Three dynamic events may occur during platoon driving: (1) vehicle joining—a vehicle joins an existing platoon, (2) vehicle leaving—a vehicle drives out of a platoon, (3) stability recovering—the platoon eliminates the extra gaps caused by vehicles leaving via changing vehicle velocities. Different events are mutually exclusive, which means only one vehicle joins or leaves the platoon in one time. We assume vehicles can only join a platoon from the end.

Four steps of vehicle joining or leaving a platoon: (1) A vehicle sends a request to the UAV. (2) The vehicle starts the operations of change driving angle or velocity after getting the approval message. Considering the vehicle joining/leaving brings a high dynamic to platoon states and only one vehicle is allowed at the same time, the approval message is necessary for our system. (3) Once finishing the actions (i.e., a vehicle in or out a platoon), the vehicle informs the UAV. (4) The UAV updates and broadcasts the platoon state to vehicles.

C. COMMUNICATION MODEL

Assuming the platoon drives on a highway, the communications between the UAV and vehicles are dominated by line-of-sight link. Thus, the channel gain between UAV and V_k is given by [20], [26], [40]

$$\begin{aligned} g_k &\approx \left(\frac{\sqrt{G}c}{4\pi f L_k}\right)^2 \\ &= \left(\frac{c}{4\pi f}\right)^2 \frac{G}{(L_k)^2} = \frac{\mathcal{A}}{H^2 + (x_k)^2} \end{aligned} \tag{2}$$

where $\mathcal{A} = G\left(\frac{c}{4\pi f}\right)^2$ indicates the unit power gain at the reference distance $L_k = 1\ m$. G represents the antenna gain. f and c are the carrier frequency and speed of light, respectively. According to the above channel model and setting $x^u < x_0^v + \frac{d}{2}$, we rank the channel gains in ascending order, i.e., $g_0 \geq g_1 \geq \cdots \geq g_K$. Both the UAV and the vehicles can obtain channel state information in our channel model.

We only consider the messages that are related to our SPA strategy. The messages from the platoon vehicles, including: (1) $\left\{x_0^v, R_0^T, d\right\}$ which is from the PL; (2) $\left\{x_k^v, R_k^T\right\}, \forall\, 1 \leq k \leq K$ which is sent by the PM, where R_k^T is the required data rate of V_k. The messages $\left\{x_0^v, \mathbb{P}, \left|\boldsymbol{V}_0^K\right|\right\}$, from the UAV, form the platoon state. Here $\mathbb{P}$ is a power matrix and represents the power allocation decision generated by UAV. The messages also contain the other platoon state data, such as speed, direction, acceleration and so on. The UAV gets the initial platoon states from the PL or the BS. The entities, including the current platoon vehicles, other platoons, non-platoon vehicles, BSs, and other UAVs, can get the broadcast messages from the UAV. Additionally, we assume the system operates in TDMA (time division multiple access) protocol.

IV. SPA STRATEGY

In this section, we first give an overview of the power allocation procedure. Then, we focus on the analysis of the proposed SPA strategy, including the capacity-power (C-P) efficiency and the rate-power (R-P) efficiency of the SPA, as the factors of cycle delay and signaling overhead have been preliminarily explained in Section I.

A. POWER ALLOCATION

Vehicles set the power based on their sequences in platoon. According to SPA strategy, the UAV generates a $\hat{K} \times \hat{K}$ power matrix $\mathbb{P} = \left\{P_{m,n} \mid 1 \leq m, n \leq \hat{K}\right\}$ where $\hat{K}$ is the maximum available platoon size constrained by the safety driving and communication requirements, and $P_{m,n} = 0$ when $m < n$. Platoon $\boldsymbol{V}_0^K$ has a power vector $\mathbb{P}\left(\left|\boldsymbol{V}_0^K\right|, :\right) = \left\{P_{\left|\boldsymbol{V}_0^K\right|,0}, P_{\left|\boldsymbol{V}_0^K\right|,1}, \cdots, P_{\left|\boldsymbol{V}_0^K\right|,K}\right\}$ where $P_{\left|\boldsymbol{V}_0^K\right|,k}$ is the power value of $V_k \in \boldsymbol{V}_0^K$ and $\left|\boldsymbol{V}_0^K\right| \leq \hat{K}$.

In a stable platoon, a vehicle switches to another power value independently when the platoon size changes. For instance, vehicles in a platoon with n members set their power based on the vector $\mathbb{P}(n, :)$. When the platoon size turns to $n+1$ after a vehicle joining, the vehicles in the new platoon change their power values based on $\mathbb{P}(n+1, :)$.

By choosing platoon $\boldsymbol{V}_0^K$ as an object of analysis, we simplify $P_{\left|\boldsymbol{V}_0^K\right|,k}$ as P_k, $0 \leq k \leq \left|\boldsymbol{V}_0^K\right|$. The transmission power of vehicles has a minimum value P^{min} and a maximum value P^{max}. As the vehicles are in the same NOMA group, the data rate r_k is equivalent to the SINR β_k with $r_k = B\log_2(1+\beta_k)$, where B is the bandwidth. Thereby, given $r_k \geq R_k^T$, we have $\beta_k \geq \beta_k^T$. Here, $R_k^T = B\log_2\left(1+\beta_k^T\right)$ and β_k^T is the required SINR of V_k.

The UAV applies the SIC decoding strategy and decodes the signals in order from the PL to the end PM. As a result, the signal of the leader is first to be decoded and has a lower outage probability [38]. The SINR of V_k is

$$\beta_k = \frac{P_k g_k}{\sum\limits_{i \in \boldsymbol{V}_{k+1}^K} P_i g_i + \sigma_N^2} = \frac{P_k^r}{I_k} \tag{3}$$

where $P_k^r = P_k g_k$ indicates the received power of V_k at the UAV; $\sigma_N^2 = NB$ is background noise where B is the bandwidth and N is the power spectral density of additive white Gaussian noise (AWGN). $I_k = \sum\limits_{i \in \boldsymbol{V}_{k+1}^K} P_i^r + \sigma_N^2$ denotes the interference-plus-noise (IpN), and specially, $I_K = \sigma_N^2$.

B. C-P EFFICIENCY

The access capacity, which means the platoon size that the system can support in this paper, depends on the SINR requirements of the users and the power of source nodes [28]. To describe the relationship between capacity and power, we first derive the formulas of P_k^r, P_k, and then achieve the C-P efficiency function.

Assuming β_k is predetermined for all the vehicles in $\boldsymbol{V}_0^K$ and according to (3), the received power of V_k can be expressed as

$$\begin{aligned} P_k^r &= \beta_k I_k \\ &\overset{(a)}{=} \beta_k\left(\beta_{k+1}+1\right) I_{k+1} \\ &\overset{(b)}{=} \beta_k \prod_{i \in \boldsymbol{V}_{k+1}^K}\left(\beta_i+1\right) I_K \\ &\overset{(c)}{=} \sigma_N^2 \beta_k \prod_{i \in \boldsymbol{V}_{k+1}^K}\left(\beta_i+1\right) \end{aligned} \tag{4}$$

where (a) is derived by

$$\begin{aligned} I_k &= \sum_{i \in \boldsymbol{V}_{k+1}^K} P_i^r + \sigma_N^2 \\ &= P_{k+1}^r + \sum_{i \in \boldsymbol{V}_{k+2}^K} P_i^r + \sigma_N^2 \\ &= P_{k+1}^r + I_{k+1} \\ &= \beta_{k+1} I_{k+1} + I_{k+1} \\ &= \left(\beta_{k+1}+1\right) I_{k+1}, \end{aligned} \tag{5}$$

(b) is achieved by iteratively utilizing (5), and (c) is derived by $I_K = \sigma_N^2$.

From (4), we know that the required received power depends only on the preset SINR of vehicles. The vehicle that closes to the end of the platoon needs a lower received power and vice versa. Also, the vehicles, whose signal decoded before V_k, need a higher received power.

In this paper, to make formulas concise, we set $\beta_k = \beta_0 \geq \beta_k^T,\ \forall\ V_k \in \boldsymbol{V}_0^K$. Thus, (4) is simplified to $P_k^r = \sigma_N^2 \beta_0 \left(\beta_0+1\right)^{K-k}$. The corresponding transmission

power of V_k is

$$\begin{aligned} P_k &= \frac{\sigma_N^2}{g_k}\beta_0\left(\beta_0+1\right)^{K-k} \\ &= P_{k+1}\lambda_{k+1} \end{aligned} \tag{6}$$

where $\lambda_{k+1} = (\beta_0+1)\frac{g_{k+1}}{g_k}$. Next, we analyze the characteristics of the transmission power by giving (7) and (8).

Assuming $\lambda_k > 1$, $V_k \in \boldsymbol{V}_0^K$, we have $P_k > P_{k+1}$ and

$$\begin{aligned} \lambda_{k+1} &= (\beta_0+1)\frac{g_{k+1}}{g_k} > 1 \\ &\overset{(a)}{\Leftrightarrow} \beta_0\left(x_k^2+H^2\right) > 2x_k d + d^2 \\ &\overset{(b)}{\Leftrightarrow} \beta_0\left(x_k-\frac{d}{\beta_0}\right)^2 > \frac{1+\beta_0}{\beta_0}d^2 - \beta_0 H^2 \\ &\overset{(c)}{\Rightarrow} \frac{1+\beta_0}{\beta_0}d^2 - \beta_0 H^2 < 0 \\ &\Leftrightarrow d < \frac{\beta_0 H}{\sqrt{1+\beta_0}} \end{aligned} \tag{7}$$

where (a) is derived by (2), (b) is derived by adding $\frac{d^2}{\beta_0}$ to both sides of the inequality, and (c) is derived by $\left(x_k-\frac{d}{\beta_0}\right)^2 \geq 0$.

Remark 1: (7) indicates that unlike the power allocation result of the conventional uplink NOMA in which a node, whose signal is decoded first, usually has a higher transmission power. The distance headway, the SINR requirement, and the altitude of UAV jointly determine which one needs a higher transmission power. For instance, when $d < \frac{\beta_0 H}{\sqrt{1+\beta_0}}$, vehicles close to the head of the platoon have higher transmission power like the conventional uplink NOMA; otherwise, the vehicle that is close to the end of platoon needs a higher transmission power when the vehicles are sparse distribution ($d \geq \frac{\beta_0 H}{\sqrt{1+\beta_0}}$). In this paper, we focus on the case of $d < \frac{\beta_0 H}{\sqrt{1+\beta_0}}$, considering the distance headway in the platoon is far lower than the height of UAV.

The transmission power of PL $P_0 = \frac{\sigma_N^2}{g_0}\beta_0\left(\beta_0+1\right)^K$ is the highest value. Thus, assuming $P_K \geq P_{min}$, the system achievable capacity is

$$\begin{aligned} &P_0 \leq P_{\max} \\ &\Rightarrow (\beta_0+1)^K \leq \frac{P_{\max} g_0}{\sigma_N^2 \beta_0} \\ &\overset{(a)}{\Rightarrow} \ln(\beta_0+1)^K \leq \ln\frac{P_{\max} g_0}{\sigma_N^2\beta_0} \\ &\Rightarrow K\ln(\beta_0+1) \leq \ln P_{\max} g_0 - \ln\sigma_N^2\beta_0 \\ &\Rightarrow K \leq \frac{\ln P_{\max} g_0 - \ln\sigma_N^2\beta_0}{\ln(\beta_0+1)} \\ &\overset{(b)}{\Rightarrow} \left|\boldsymbol{V}_0^K\right| \leq \frac{\ln P_{\max} g_0 - \ln\sigma_N^2\beta_0}{\ln(\beta_0+1)} + 1 \end{aligned} \tag{8}$$

where (a) is derived by taking the logarithm on both sides of the inequality, and (b) is derived by $\left|\boldsymbol{V}_0^K\right| = K+1$.

Remark 2: (8) indicates that the access capacity depends on P_{max}, β_0 and the channel gain g_0. A higher transmission power of vehicle, a higher system achievable capacity is achieved, while the SINR of vehicles and the position of UAV are fixed. On the contrary, the increase of required SINR will limit the capacity. Thus, assigning vehicles to several NOMA channels is necessary when the platoon size is large. In this paper, we consider the scenario of grouping one platoon into a single group.

Though the access capacity of the proposed NOMA system is growing with the increasing of the available transmission power of PL, unlimited increase in transmission power is unpractical. Thus, we define the C-P efficiency by

$$\begin{aligned} \eta &= \frac{K+1}{P_0} \\ &= \frac{K+1}{\frac{\sigma_N^2}{g_0}\beta_0\left(\beta_0+1\right)^K} \\ &= \frac{g_0(K+1)}{\sigma_N^2\beta_0\left(\beta_0+1\right)^K}, \end{aligned} \tag{9}$$

and present how the C-P efficiency changes with the platoon size with the following theorem:

Theorem 1: The C-P efficiency decreases with the growing of the platoon size under the case with $\beta_0 \geqslant \sqrt{e}-1$.

Proof: Extract the part related to K from (9), and define a function

$$f(K) = \frac{K+1}{(\beta_0+1)^K}. \tag{10}$$

The first-order derivative of (10) is given by

$$\begin{aligned} f'(\mathrm{K}) &= \left(\frac{\mathrm{K}+1}{(\beta_0+1)^K}\right)' \\ &= \frac{1-(K+1)\ln(\beta_0+1)}{(\beta_0+1)^{\mathrm{K}}}. \end{aligned} \tag{11}$$

Set $f'(K) < 0$, we get

$$K > \frac{1}{\ln(\beta_0+1)} - 1. \tag{12}$$

A platoon has at least two vehicles, thus we have $K > 1$. Thereby, following from $\frac{1}{\ln(\beta_0+1)} - 1 \leq 1$, (12) is obtained, where $\frac{1}{\ln(\beta_0+1)} - 1 \leq 1$ and $\beta_0 \geq \sqrt{e}-1$ are equivalent. □

Theorem 1 indicates that an optimal C-P efficiency exists as the platoon size increase with a small required SINR which satisfies $\beta_0 < \sqrt{e}-1$. Otherwise, when $\beta_0 \geq \sqrt{e}-1$, the C-P efficiency keeps decreasing.

C. R-P EFFICIENCY

To achieve the expression of R-P efficiency, we firstly give the platoon total transmission power $\boldsymbol{P}$ and the system data rate R, respectively.

Using (6), we obtain

$$\boldsymbol{P} = \sum_{k\in\boldsymbol{V}_0^K} P_k$$

$$= \sigma_N^2 \beta_0 \sum_{k \in \boldsymbol{V}_0^K} \frac{(\beta_0+1)^{K-k}}{g_k}. \tag{13}$$

According to (2), g_k is highly related to the vehicle position and can be calculated mathematically by giving the platoon size and the distance headway.

Remark 3: The overall power consumption increases with the increase of platoon size, which means that the more vehicles in the platoon, the more power-consuming. According to (2) and (6), if the platoon size is fixed, a larger distance headway d leads to a higher transmission power. To reduce the power consumption, we need to decrease d. However, a platoon with small d requires a high QoS, i.e., a higher SINR is required to further decrease the outage probability to achieve a lower latency, and a large β_0 brings a high transmission power [16]. Instead of achieving a trade-off, in this paper, we focus on designing a power allocation strategy constrained by the preset SINR.

Following form (3), the system overall data rate can be expressed as

$$\begin{aligned}
R &= \sum_{k \in \boldsymbol{V}_0^K} r_k \\
&= \sum_{k \in \boldsymbol{V}_0^K} B \log_2 \left(1 + \frac{P_k^r}{\sum_{i \in \boldsymbol{V}_{k+1}^K} P_i^r + \sigma_N^2}\right) \\
&\overset{(a)}{=} B \sum_{k \in \boldsymbol{V}_0^K} \left\{ \log_2 \left(P_k^r + \sum_{i \in \boldsymbol{V}_{k+1}^K} P_i^r + \sigma_N^2 \right) \right. \\
&\quad \left. - \log_2 \left(\sum_{i \in \boldsymbol{V}_{k+1}^K} P_i^r + \sigma_N^2 \right) \right\} \\
&= B \sum_{k \in \boldsymbol{V}_0^K} \left\{ \log_2 \left(\sum_{i \in \boldsymbol{V}_k^K} P_i^r + \sigma_N^2 \right) \right. \\
&\quad \left. - \log_2 \left(\sum_{i \in \boldsymbol{V}_{k+1}^K} P_i^r + \sigma_N^2 \right) \right\} \\
&\overset{(b)}{=} B \left\{ \log_2 \left(\sum_{i \in \boldsymbol{V}_0^K} P_i^r + \sigma_N^2 \right) - \log_2 \sigma_N^2 \right\} \\
&\overset{(c)}{=} B \log_2 \left(1 + \frac{\sum_{i \in \boldsymbol{V}_0^K} P_i^r}{\sigma_N^2}\right) \\
&\overset{(d)}{=} B \log_2 \left(1 + \frac{\sum_{i \in \boldsymbol{V}_0^K} \sigma_N^2 \beta_0 (\beta_0+1)^{K-i}}{\sigma_N^2}\right) \\
&= B \log_2 \left(1 + \beta_0 \sum_{i \in \boldsymbol{V}_0^K} (\beta_0+1)^{K-i}\right).
\end{aligned} \tag{14}$$

Here, (a) and (c) are derived using $\log_2 \frac{x}{y} = \log_2 x - \log_2 y$, $x, y > 0$, (b) is achieved via telescoping sum, (d) follows from the simplified form of (4) in Section IV-B. Specially, $\sum_{V_k \in \boldsymbol{V}_0^K} P_k^r$ represents the total received power at the UAV.

Remark 4: The system data rate is the overall vehicle data rate in the platoon. In (14), we can observe that the data rate of the system is relevant to the total received power at the UAV. In other words, all vehicles act as one "node" which sends signals to the UAV through multiple antennas. Theoretically, if every vehicle sends signals with the maximum power, the system data rate will reach the upper bound. However, constrained by the required SINR and the SIC mechanism, we set vehicle power mainly according to (6).

As mentioned above, the transmission power of vehicles is the only factor affecting the total data rate of the platoon. Thus, using (13) and (14), we define R-P efficiency as

$$\phi = \frac{R}{\boldsymbol{P}} = \frac{B \log_2 \left(1 + \beta_0 \sum_{i \in \boldsymbol{V}_0^K} (\beta_0+1)^{K-i}\right)}{\sigma_N^2 \beta_0 \sum_{k \in \boldsymbol{V}_0^K} \frac{(\beta_0+1)^{K-k}}{g_k}}. \tag{15}$$

Remark 5: Recall that the power value of vehicles are related to the platoon states. Therefore, the total transmission power and system data rate will be fixed once the platoon size and required SINR are determined. As observed from (15), the R-P efficiency changes with K and β_0.

V. PLATOON CHANGING

In this section, we analyze the performance of the proposed SPA strategy in dynamic environments, including the cases of the UAV moving, vehicle joining and leaving, and platoon adjusting.

A. UAV MOVING

In this subsection, the expression of the platoon total transmission power with respect to the UAV position is given and the SINR variation is analyzed. "UAV moving" here means the change of the relative horizontal distance between the UAV and the platoon.

1) POWER CONSUMING

Using (1) and (6) and setting $x_0^v = 0$, we get

$$\begin{aligned}
P_k &= \frac{\sigma_N^2}{g_k} \beta_0 (\beta_0+1)^{K-k} \\
&\approx \frac{\sigma_N^2}{\mathcal{A}} \beta_0 (\beta_0+1)^{K-k} \left(H^2 + (x_k)^2\right) \\
&= \frac{\sigma_N^2}{\mathcal{A}} \beta_0 (\beta_0+1)^{K-k} \left(H^2 + \left(x^u - k \cdot d\right)^2\right).
\end{aligned} \tag{16}$$

From (16), we know that P_k is minimized when the UAV is directly above V_k with $x^u = k \cdot d$.

The total transmission power of the platoon is expressed as below by using (13)

$$\boldsymbol{P} \approx \frac{\sigma_N^2 \beta_0}{\mathcal{A}} \sum_{k \in \boldsymbol{V}_0^K} (\beta_0 + 1)^{K-k} \left(H^2 + \left(x^u - k \cdot d \right)^2 \right). \quad (17)$$

Theorem 2: Giving $\beta_0 > 1$ and fixing the UAV height H, to minimize the total transmission power, the abscissa value of UAV should satisfy $0 < x^u < d$.

Proof: Detailed proof can be found in Appendix A. □

Theorem 2 indicates that the UAV should be deployed between the first two vehicles of a platoon to minimize the total power, which meets the assumption of $x_u < x_0^v + \frac{d}{2}$. For calculation convenience, we set $x_u = x_0^v = 0$ in the following analysis.

2) SINR CHANGING

The SINR of V_k with respect to x_k is

$$\begin{aligned} \beta_k(x_k) &= \frac{P_k g_k}{\sum\limits_{i \in \boldsymbol{V}_{k+1}^K} P_i g_i + \sigma_N^2} \\ &= \frac{P_k}{\sum\limits_{i \in \boldsymbol{V}_{k+1}^K} P_i \frac{g_i}{g_k} + \frac{\sigma_N^2}{g_k}} \\ &\approx \frac{P_k}{\sum\limits_{i \in \boldsymbol{V}_{k+1}^K} P_i \frac{H^2 + (x_k)^2}{H^2 + (x_i)^2} + \frac{\sigma_N^2 \cdot (H^2 + (x_k)^2)}{\mathcal{A}}} \\ &= \frac{P_k}{\Gamma(x_k, k)} \end{aligned} \quad (18)$$

where

$$\Gamma(x_k, k) = \sum_{i \in \boldsymbol{V}_{k+1}^K} P_i w(x_k, k, i) + \frac{\sigma_N^2 \left(H^2 + (x_k)^2 \right)}{\mathcal{A}}, \quad (19)$$

and

$$\begin{aligned} w(x_k, k, i) &= \frac{H^2 + (x_k)^2}{H^2 + (x_i)^2} \\ &= \frac{H^2 + (x_k)^2}{H^2 + (x_k + (i-k)d)^2}. \end{aligned} \quad (20)$$

Remark 6: We can figure out how the SINR of vehicles varies with the movement of UAV by using (18), when all the vehicles' transmission power are fixed.

Lemma 1: $\Gamma(x_k, k)$ and $w(x_k, k, i)$ are lower convex functions when $x_k < \sqrt{\left(\frac{d}{2}\right)^2 + H^2} - \frac{d}{2}$ and are monotonically increasing functions when $x_k \geq \sqrt{\left(\frac{d}{2}\right)^2 + H^2} - \frac{d}{2}$.

Proof: Detailed proof can be found in Appendix B. □

From Lemma 1, we know that given $x_k \in \langle x^0, x^1 \rangle$, $0 \leq x^0 < x^1$, if the extreme point of $\Gamma(x_k, k)$ exists, then this point $x^p \leq \sqrt{\left(\frac{d}{2}\right)^2 + H^2} - \frac{d}{2}$ is unique and $\Gamma(x^p, k) \leq \Gamma(x_k, k)$; otherwise, $\Gamma(x_k, k)$ is a monotonic function. Thus we always have $\Gamma(x_k, k) \leq \max\left\{\Gamma(x^0, k), \Gamma(x^1, k)\right\}$ with $x_k \in \langle x^0, x^1 \rangle$.

Theorem 3: With $x_k \in \langle x^0, x^1 \rangle$, $0 \leq x^0 < x^1$, we have $\beta_k(x_k) \geq \min\left\{\beta_k(x^0), \beta_k(x^1)\right\}$.

Proof: Assuming $\Gamma(x^1, k) \geq \Gamma(x^0, k)$, for $x_k \in \langle x^0, x^1 \rangle$, we have

$$\begin{aligned} \beta_k(x_k) &= \frac{P_k}{\Gamma(x_k, k)} \geq \frac{P_k}{\max\left\{\Gamma(x^0, k), \Gamma(x^1, k)\right\}} \\ &= \frac{P_k}{\Gamma(x^1, k)} = \beta_k(x^1) = \min\left\{\beta_k(x^0), \beta_k(x^1)\right\}. \end{aligned}$$

Similarly, we can get the same results for the case with $\Gamma(x^1, k) < \Gamma(x^0, k)$. □

Set $\beta_k(x^1) = \beta_0$ and following from Theorem 3, we obtain $\beta_k(x_k) \geq \beta_0$ with $\beta_k(x^1) = \min\left\{\beta_k(x^0), \beta_k(x^1)\right\}$. Thus, when x_k decreases from x^1 to x^0, vehicle k will have an SINR that is always greater than or equal to β_0. If $\beta_k(x^0) = \min\left\{\beta_k(x^0), \beta_k(x^1)\right\}$, we have $\beta_k(x^0) < \beta_k(x^1) = \beta_0$. Thereby, the SINR of vehicle k will be less than β_0, especially for the case with $x^1 \leq x^p$.

B. VEHICLE JOINING AND LEAVING

In this subsection, the vehicle SINR is analyzed in following two cases: A new vehicle joining the platoon, and one vehicle leaving the platoon.

1) VEHICLE JOINING

As only one vehicle is allowed to join the platoon from the end at once, we note the new vehicle as V_{K+1} which joins an existing platoon $\boldsymbol{V}_0^K$ (the original platoon), thus $\boldsymbol{V}_0^K \bigcup V_{K+1} = \boldsymbol{V}_0^{K+1}$ (the new platoon), $K + 1 \leq \hat{K}$. The SINR of $V_k \in \boldsymbol{V}_0^K$ changes with the new vehicle joining is

$$\begin{aligned} \beta_k' &= \frac{P_k g_k}{\sum_{i \in \boldsymbol{V}_{k+1}^{K+1}} P_i g_i + \sigma_N^2} \\ &= \frac{P_k g_k}{\sum_{i \in \boldsymbol{V}_{k+1}^{K}} P_i g_i + \sigma_N^2 + P_{K+1} g_{K+1}} \\ &= \frac{P_k^r}{I_k + P_{K+1} g_{K+1}} = \frac{\beta_k I_k}{I_k + P_{K+1} g_{K+1}} \\ &= \frac{\beta_k}{1 + \frac{P_{K+1} g_{K+1}}{I_k}} < \beta_k. \end{aligned} \quad (21)$$

From (21), we know that the SINR of vehicles that belong to the original platoon decreases with the new vehicle joining.

2) VEHICLE LEAVING

Assuming the leaving vehicle is $V_{k'} = k', 0 \le k' \le K$. For $V_k \in \boldsymbol{V}_0^{k'-1}$, the SINR can be expressed as

$$\begin{aligned}\beta_k'' &= \frac{P_k g_k}{\sum_{i\in \boldsymbol{V}_{k+1}^K} P_i g_i - P_{k'} g_{k'} + \sigma_N^2} \\ &= \frac{P_k^r}{I_k - P_{k'} g_{k'}} \\ &= \frac{\beta_k}{1 - \frac{P_{k'} g_{k'}}{I_k}} > \beta_k, \end{aligned} \tag{22}$$

which means that all these vehicles get a higher SINR.

For $V_k \in \boldsymbol{V}_{k'+1}^K$, according to (3), the SINR remains constant with unchanged I_k and P_k.

C. PLATOON ADJUSTING

The platoon needs to eliminate the extra gap caused by vehicle leaving, except the leaving vehicle is at the end of platoon. In this subsection, we analyze the changes in SINR of two types of vehicles which are $V_k \in \boldsymbol{V}_0^{k'-1}$ and $V_k \in \boldsymbol{V}_{k'+1}^K$. And then, a transmission power changing principle is proposed via Theorem 4 to maintain the vehicle SINR not lower than the present value during the platoon adjusting period.

The vehicle SINR is affected by the received power P_k^r, $\forall\ V_k \in \boldsymbol{V}_0^K$, and the IpN, according to (3). For $V_k \in \boldsymbol{V}_0^{k'-1}$, the P_k^r remains constant since the unchanged relative position x_k. On the contrary, for $V_k \in \boldsymbol{V}_{k'+1}^K$, the P_k^r increases due to the decrease of x_k. However, changes in IpN are complex. For instance, in the case of $V_k \in \boldsymbol{V}_0^{k'-1}$, the IpN decreases with $V_{k'}$ left, but increases with the increasing P_k^r, $V_k \in \boldsymbol{V}_{k'+1}^K$. Thus, for this case, a detail analyses of IpN is carried out in Appendix C, and we get the conclusion that the SINR of vehicles in $\boldsymbol{V}_0^{k'-1}$ is increasing.

For $V_k \in \boldsymbol{V}_{k'+1}^K$, according to Section V-A, the vehicles after the leaving vehicle can be seen as the sub-platoon $\boldsymbol{V}_{k'+1}^K$ moving to the UAV, which may result in SINR decreasing. Thus, vehicles need to change their power according to the below theorem.

Theorem 4: The changed power of V_k should satisfy $\max\left\{\frac{P_{k-1}}{\lambda_k}, \frac{P_{k-1}}{\lambda_{k+1}}\right\} \le P_k' \le P_{k-1}$

Proof: Detailed proof can be found in Appendix E. □

VI. STRATEGY IMPLEMENTATION

Above analysis shows that the SINR of vehicles changes over different platoon dynamic events, and the SINR will be attenuated in some cases. Therefore, we design two algorithms, the power-reserved algorithm, and the power-moving algorithm, to ensure the value of real-time SINR is not lower than β_0. The power-reserved algorithm is for the stable platoon situations. "power-reserved" means that vehicles in a stable platoon set transmission power by assuming the platoon already having a new PM, and the transmission power of the vehicle that tries to join the platoon is reserved. As a result, the SINR of vehicles in the platoon will not fall below β_0 for new vehicle joining. The power-moving algorithm is for the dynamic platoon, where "power moving" means that some vehicles in the platoon change transmission power into a higher level by supposing the platoon has reached the stable state. In this section, we first describe the overall system power allocation procedure and then introduce the two algorithms.

Algorithm 1 System Power Allocation

Input: $H_0, \beta_0, d, \boldsymbol{V}$
Output: $\boldsymbol{P}$

1: **Initial**: $n = 0, \boldsymbol{P} = 0$
2: **while** $H = H_0$ **do**
3: UAV updates $\mathbb{P}$;
4: **if** UAV reveiced a confirmation message from a vehicle $V_{k'}$ that just left the platoon **then**
5: $f_{left} = V_{k'}$;
6: $\boldsymbol{V} \leftarrow \boldsymbol{V}/V_{k'}$;
7: **else**
8: $f_{left} = -1$;
9: **end if**
10: **if** UAV reveived a confirmation message for a vehicle V_{new} that completing the joining process **then**
11: $V_{new} = |\boldsymbol{V}|, \boldsymbol{V} \leftarrow \boldsymbol{V} \cup V_{new}$;
12: **end if**
13: UAV broadcasts $\boldsymbol{V}$ and $\mathbb{P}$ to vehicles;
14: **if** $f_{left} == -1$ **and** $\forall V_k \in \boldsymbol{V}, x_{k+1} - x_k = d$ **then**
15: Vehicles and UAV update the sequence numbers;
16: To Algorithm 2;
17: **else**
18: To Algorithm 3;
19: **end if**
20: **end while**

A. SYSTEM POWER ALLOCATION

The proposed power allocation strategy (Algorithm 1) is executed after the deployment of the UAV—the UAV reaches the predefined height H_0: $H = H_0$. The UAV obtains the values of H_0, β_0, and d from the PL. The UAV updates the platoon states and power matrix at every beginning of the algorithm. As shown in steps 3-12 of Algorithm 1, the symbol f_{left} indicates whether a vehicle has left the platoon. The UAV broadcasts the platoon state (including the x_0^u) and $\mathbb{P}$ to the vehicles before vehicles update their power. The system turns to the power-moving algorithm (Algorithm 3) when the left flag f_{left} is greater than -1 and/or any of the distance headway is beyond d. Otherwise, the system goes to the power-reserved algorithm (Algorithm 2).

B. POWER ALLOCATION OF STABLE PLATOON

In this subsection, we describe the details of our power-reserved algorithm. Especially, "power reserved" is further explained as follows: For platoon $\boldsymbol{V}_0^K$, vehicles set transmission power according to $\mathbb{P}(K+2, :)$ instead of $\mathbb{P}(K+1, :)$, and $P_{K+2,K+1}$ is the reserved power for the new vehicle

Algorithm 2 Power-Reserved Algorithm

Input: $\boldsymbol{V}$
Output: $\boldsymbol{P}$
1: **if** UAV received a joining request **then**
2: $n = |\boldsymbol{V}| + 1$;
3: **else**
4: $n = |\boldsymbol{V}|$;
5: **end if**
6: UAV broadcasts n to vehicles;
7: **for** $\forall V_k \in \boldsymbol{V}$ **do**
8: $P_k = P_{n,k}$;
9: **end for**

V_{K+1}. The UAV sets the platoon size manually after receiving a joining request. As shown in steps 7-9 of Algorithm 2, the vehicles start to update their power after getting a new platoon size n from the UAV. The time complexity of updating power for vehicles in platoon $\boldsymbol{V}$ is $\mathcal{O}(|\boldsymbol{V}|^2)$, $|\boldsymbol{V}| \leq \hat{K}$.

However, the reserving-power mechanism causes additional power consuming as all vehicles increasing transmission power. We calculate the additional power cost $\boldsymbol{P}_a^t$ by subtracting $\boldsymbol{P}_1^t$ from $\boldsymbol{P}_0^t$, where $\boldsymbol{P}_1^t$ and $\boldsymbol{P}_0^t$ are the total power of platoon with power reserving and the total power of the platoon without power reserving respectively.

$$\begin{aligned}\boldsymbol{P}_a^t &= \boldsymbol{P}_1^t - \boldsymbol{P}_0^t \\ &= \sigma_N^2\beta_0 \sum_{k\in\boldsymbol{V}_0^K} \frac{(\beta_0+1)^{K+1-k}}{g_k} \\ &\quad - \sigma_N^2\beta_0 \sum_{k\in\boldsymbol{V}_0^K} \frac{(\beta_0+1)^{K-k}}{g_k} \\ &= (\beta_0+1-1)\,\sigma_N^2\beta_0 \sum_{k\in\boldsymbol{V}_0^K} \frac{(\beta_0+1)^{K-k}}{g_k} \\ &= \beta_0\sigma_N^2\beta_0 \sum_{k\in\boldsymbol{V}_0^K} \frac{(\beta_0+1)^{K-k}}{g_k} \\ &= \beta_0 \boldsymbol{P}_0^t. \end{aligned} \tag{23}$$

From (23), we know that the additional power becomes great with the increase of SINR and platoon size. For instance, the more vehicles joining in a platoon (according to (13)) and/or the higher system required SINR, the more additional power cost is generated. Meanwhile, with the additional power, the SINR of vehicles in original platoon is larger than β_0 (according to (3)). If there are no available links for the new vehicle to send request messages, our system will reserve power all the time, and the new vehicle can communicate with the UAV on the NOMA channel.

C. DYNAMIC POWER ALLOCATION

In this subsection, the power-moving algorithm is introduced for dynamic power allocation. In the power-moving algorithm, we try to reduce the number of vehicles that need to change the power and the signaling overhead. Thus, on the one hand, we fix the transmission power of vehicles belonging to $\boldsymbol{V}_0^{k'-1}$, according to the analysis of Section V-C. On the other hand, Section V-A2 indicates that not all the vehicles belonging $\boldsymbol{V}_{k'+1}^K$ surfer SINR decreasing. Therefore, we find the vehicle $V_l = l$ whose SINR is decreasing and has the largest sequence number in $\boldsymbol{V}_{k'+1}^K$ using (18), considering all the other vehicles $V_k \in \boldsymbol{V}_{k'+1}^K$, $l < k < k'$ will change power like V_l. As a result, the number of vehicles that need to change power is $\left(k' - l\right)$. We call V_l the first vehicle which needs to change transmission power.

To reduce the calculation complexity, we simplify above power change condition (having decreasing SINR) by using below function:

$$\begin{aligned}\Delta_w^{k,i} &= w(x_k - d, k, i) - w(x_k, k, i) \\ &= \frac{H^2 + (x_k - d)^2}{H^2 + (x_k - d + (i-k)\cdot d)^2} \\ &\quad - \frac{H^2 + (x_k)^2}{H^2 + (x_k + (i-k)\cdot d)^2}\end{aligned} \tag{24}$$

where $i > k$ and $\Delta_w^{k,i}$ means the variation of weight of P_i in (18). $\exists i$, $\Delta_w^{k,i} > 0$ means the corresponding item in (19) is increasing with the platoon adjusting, and we think the vehicle needs to change its power.

Another way to reduce the signaling overhead is that the vehicles in $\boldsymbol{V}_{k'+1}^l$ only change their power once during the platoon adjusting. Based on Theorem 4, the vehicles in $\boldsymbol{V}_{k'+1}^l$ reset their power to the power of their adjacent front vehicles respectively via "power moving". Fig. 3 illustrates the power-moving details: $\boldsymbol{V}$ is a stable platoon with 10 vehicles, and $\boldsymbol{V}/V_4$ is a platoon that without the left vehicle V_4; $V_l = V_8$. Thus, $P_4 \sim P_7$ (the power values of $V_4 \sim V_7$) in $\boldsymbol{V}$ "move" one step back to be the power values of $V_5 \sim V_8$ in $\boldsymbol{V}/V_4$. Algorithm 3 shows the power-moving process, where line 7 to 11 execute the power- moving.

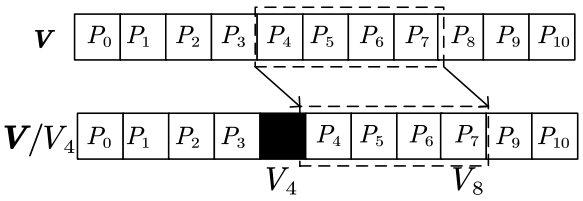

FIGURE 3. Power moving.

Next, we prove that the vehicle SINR are guaranteed under the proposed power-moving algorithm, which is started by giving a lemma as below:

Lemma 2: The total received power at UAV of sub-platoon $\boldsymbol{V}_{k'+1}^K$ satisfies

$$\textstyle\sum_{j\in\boldsymbol{V}_{k'+1}^K} P_j' g_j' < \sum_{j\in\boldsymbol{V}_{k'}^K} P_j g_j.$$

Here, $P_j' = P_{j-1}$ and g_j' is the channel gain of $V_j \in \boldsymbol{V}_{k'+1}^K$ during platoon adjusting period.

Proof: Detailed proof can be found in Appendix D. □

Algorithm 3 Power-Moving Algorithm

Input: $\boldsymbol{V}, V_{k'}, f_{left}$
Output: $\boldsymbol{P}$

```
n = |V|;
if f_left ≠ −1 then
    for V (V_k > V_k') do
        Use (24) to find the vehicle V_l that first changing its power;
    end for
    UAV broadcasts "l";
    if V_k' < k ≤ V_l then
        P_k = P_{n,k−1};
    else
        P_k = P_{n,k};
    end if
end if
```

Based on Lemma 2, for $V_j \in \boldsymbol{V}_0^{k'-1}$, the vehicle SINR with power-moving algorithm is expressed as

$$\begin{aligned}\beta_j' &= \frac{P_j^r}{\sum_{i\in\boldsymbol{V}_{j+1}^{k'-1}} P_i g_i + \sum_{i\in\boldsymbol{V}_{k'+1}^{K}} P_i' g_i' + \sigma_N^2} \\ &> \frac{P_j^r}{\sum_{i\in\boldsymbol{V}_{j+1}^{k'-1}} P_i g_i + \sum_{i\in\boldsymbol{V}_{k'}^{K}} P_i g_i + \sigma_N^2} \\ &= \frac{P_j^r}{\sum_{i\in\boldsymbol{V}_{j+1}^{K}} P_i g_i + \sigma_N^2} \\ &= \frac{P_j^r}{I_j} = \beta_j. \end{aligned} \tag{25}$$

(25) indicates that the SINR of vehicles belong to sub-platoon $\boldsymbol{V}_0^{k'-1}$ is greater than its initial value. Consider $\beta_j = \beta_0, \forall\, V_j \in \boldsymbol{V}_0^k$, we have $\beta_j' > \beta_0, V_j \in \boldsymbol{V}_0^{k'-1}$. For $V_j \in \boldsymbol{V}_{k'+1}^K$, we can prove that $\beta_j' \geq \beta_0$. The detailed proof can be found in Appendix E.

Remark 7: Though designed for vehicles joining a platoon from the end, the above algorithms can also handle vehicles joining a platoon from the middle. If the sequence numbers and power values of all the vehicles remain unchanged after a vehicle leaving the platoon, a new vehicle can join the platoon by directly replacing the leaving vehicle. Otherwise, the platoon needs to generate a position and reserve the power resource for the new vehicle via moving a sub-platoon. Here, the sub-platoon moving is the inverse process of the platoon adjusting: (1) Vehicles in the original platoon change their power according to the power-reserved algorithm, (2) and then the sub-platoon increases the distance to the adjacent front vehicle via velocity changing. (3) Vehicles in the sub-platoon decrease their transmission power in an inverse power-moving manner after the platoon obtains the required "gap". As a result, the platoon is in the state that assuming a new vehicle has joined the platoon.

TABLE 2. Parameters configuration.

Parameter	Value	Parameter	Value
H	100 m	d	10 m
Platoon size	12	k'	5
B	1 MHz	G_l	1
f	6 GHz	c	3.0×10^8 m/s
N	-174 dbm/Hz	x_u, x_0^v	0
l	11	P_{max}	1∼20 W

VII. SIMULATION RESULTS

In this section, the performance of the proposed SPA strategy is evaluated using extensive simulations. Subsection VII-A provides the simulation setup. In subsection VII-B, the performance is evaluated in terms of access capacity, C-P efficiency, and R-P efficiency. We evaluate the performance of our proposed dynamic power allocation in guaranteeing the required SINR in subsection VII-C.

A. SIMULATION SETUP

We consider a platoon with 12 vehicles, the distance headway is set to 10 meters, and the maximum transmission power is selected in the range of 1 ∼ 20 W [12], [40]. We set the carrier frequency and bandwidth as 6 GHz and 1 MHz, respectively [23]. The velocity set of vehicles is omitted, consider our SPA strategy is related to the relative position of vehicles. Meanwhile, given a distance headway, the platoon usually have a certain speed [17]. Also, we set the abscissa of UAV and PL to 0. Important parameters are listed in Table 2.

B. EVALUATION OF SPA STRATEGY

Figure 4 shows the access capacity of SPA in terms of different maximum vehicle transmission power. It is obvious

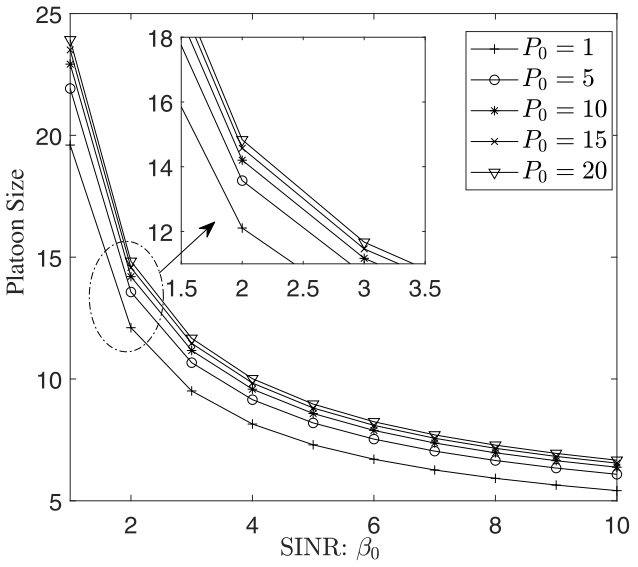

FIGURE 4. The access capacity performance of SPA in terms of different maximum vehicle transmission power.

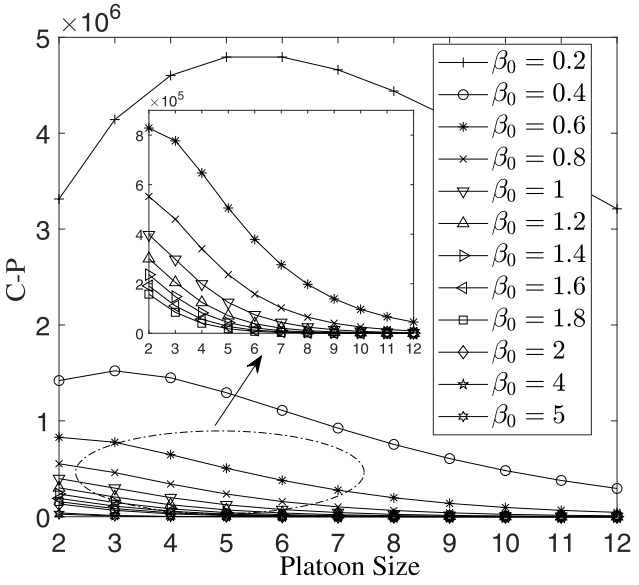

FIGURE 5. C-P efficiency varying with the platoon size under different SINR values.

that a larger P_0 supports more vehicles to share one channel. However, with the P_0 increasing tenfold, such as from 1 W to 10 W, the increment of system capacity is less than 17%. What's more, the increment of system capacity decreases with P_0 increase. Fig. 4 also indicates that the capacity drops with the SINR increasing for a fixed transmission power.

In Figs. 5 and 6, we evaluate the impact of SINR and platoon size on the C-P efficiency and the R-P efficiency respectively. Fig. 5 shows that we can get an optimized C-P efficiency by growing platoon size with a small β_0, for instance, when the platoon size equals 5 and $\beta_0 = 0.2$, the C-P efficiency is maximized. However, we can not achieve a platoon size maximizing the C-P efficiency with the event $\beta_0 \leq \sqrt{e} - 1$, which is consistent with Theorem 1. As shown in the internal subfigure of Fig. 5, the C-P efficiency decreases with the increase of platoon size when $\beta_0 \leq 0.6$. To facility the transmission reliability, we set $\beta_0 > 1$ in this paper. Similarly, in Fig. 6, the R-P efficiency falls sharply with platoon size increasing, and a higher value of SINR brings a lower R-P efficiency.

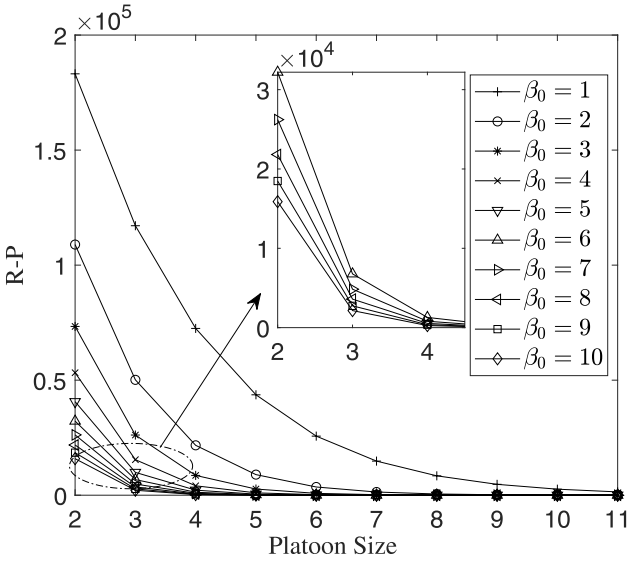

FIGURE 6. R-P Efficiency varying with the platoon size under different SINR values.

C. SINR PERFORMANCE OF DYNAMIC POWER ALLOCATION

In Fig. 7 and Fig. 8, we evaluate the performance of our dynamic power allocation during platoon adjusting. According to the results in Fig. 4, we know that increasing transmission power does not expand the access capacity obviously, thus, we set the vehicle transmission power to 5 W. By setting SINR equals 3, we get the corresponding platoon size 11. "FP" denotes fixed power, which means vehicles do not

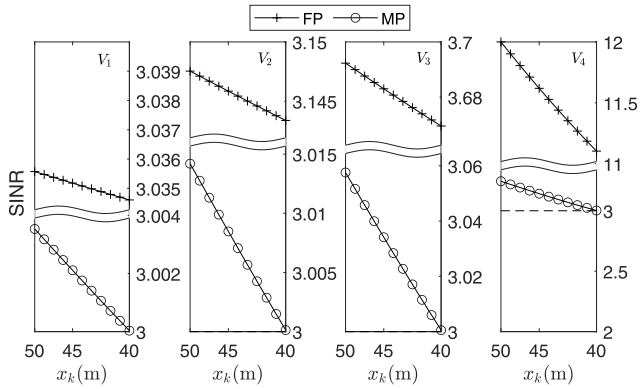

FIGURE 7. The performance of vehicle SINR under different power changing strategies (V_1-V_4).

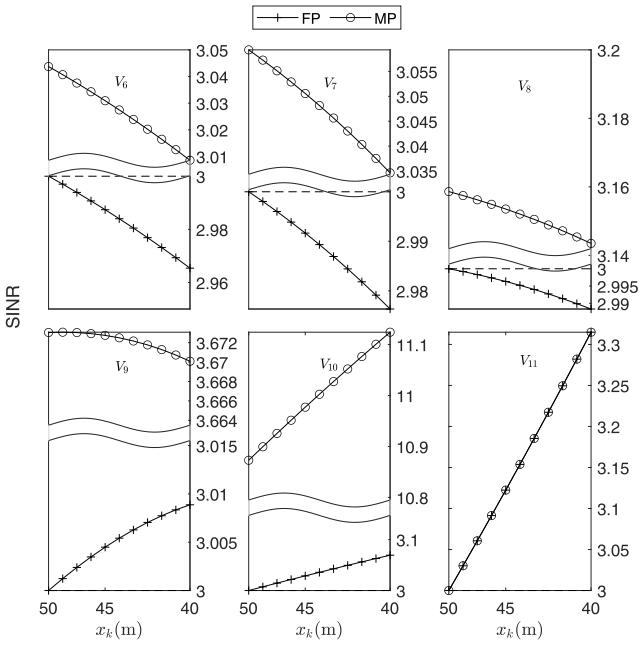

FIGURE 8. The performance of vehicle SINR under different power changing strategies (V_6-V_{11}).

change their power when there is a leaving vehicle; "MP" denotes moving power, which means vehicles change their power according to the proposed moving-power algorithm.

Figure 7 shows that the SINR of the vehicles ahead of the leaving vehicle are always larger than 3, even though the SINR performance of MP is lower than that of FP. On the contrary, Fig. 8 shows that the SINR of vehicles behind the leaving vehicle gets larger with the moving-power algorithm. Especially, V_{11}, the end vehicle of the platoon, has a growing SINR when moving to the UAV, because of no additional interference from the other vehicles and the unchanged power. V_{10} has the largest MP SINR, as to be the "first" vehicle that changes power. Fig. 8 also shows that the "first" vehicle should be V_8, as the FP SINR of V_9 and V_{10} increases with decreasing x_k, which is the error from our simplified condition.

VIII. CONCLUSION

In this paper, we have investigated the power allocation problem in a UAV-aided platoon communication system. To achieve an efficient power control scheme, we propose an SPA strategy, including a power-reserved algorithm and a power-moving algorithm. The proposed SPA strategy reduces the signaling overhead on power controls, where the system only needs to maintain the updating of platoon status to control vehicle transmission power. The upper bound of vehicle transmission power and the SINR requirement limit the number of vehicles grouped into one channel. Therefore, we need to make several groups for a platoon and use multiple channels, by carefully designing the number of vehicles in every NOMA channel. We will research the grouping strategy in our future work.

APPENDIX A

Proof of Theorem 2. Firstly, we transform (17) into a function of x^u, i.e.,

$$\mathcal{P}\left(x^u\right) = \sum_{k\in \boldsymbol{V}_0^K} (\beta_0+1)^{K-k}\left(H^2+\left(x^u-k\cdot d\right)^2\right). \quad (26)$$

Then, to find the extreme value, the first-order derivative of (26) is given by

$$\begin{aligned}\mathcal{P}'\left(x^u\right) &= \left(\sum_{k\in \boldsymbol{V}_0^K} (\beta_0+1)^{K-k}\left(H^2+\left(x^u-k\cdot d\right)^2\right)\right)'\\ &= \sum_{k\in \boldsymbol{V}_0^K} (\beta_0+1)^{K-k}\, 2\left(x^u-k\cdot d\right)\\ &= 2\left(\beta_0+1\right)^K\left(\sum_{k\in \boldsymbol{V}_0^K} (\beta_0+1)^{-k}\left(x^u-k\cdot d\right)\right)\\ &= 2a^{-K}\left(\sum_{k\in \boldsymbol{V}_0^K} a^k x^u - d\sum_{k\in \boldsymbol{V}_0^K} a^k k\right), \end{aligned} \quad (27)$$

where $\alpha = \frac{1}{\beta_0+1}$.

Set $\mathcal{P}' = 0$ and using (29), we get

$$\begin{aligned} x^u &= d\frac{\sum\limits_{k\in \boldsymbol{V}_0^K}\alpha^k k}{\sum\limits_{k\in \boldsymbol{V}_0^K}\alpha^k}\\ &= d\frac{\alpha-\alpha^{K+1}-K a^{K+1}(1-\alpha)}{\left(1-\alpha^{K+1}\right)(1-\alpha)}\\ &\overset{(a)}{<} d. \end{aligned} \quad (28)$$

Here, (a) follows from the following derivation

$$\begin{aligned} &\frac{\alpha-\alpha^{K+1}-K a^{K+1}(1-\alpha)}{\left(1-\alpha^{K+1}\right)(1-\alpha)}\\ &= \frac{\alpha-\alpha^{K+1}-K\alpha^{K+1}+K\alpha^{K+2}}{1-\alpha-\alpha^{K+1}+\alpha^{K+2}}\\ &< \frac{1-\alpha-\alpha^{K+1}-K\alpha^{K+1}+K\alpha^{K+2}}{1-\alpha-\alpha^{K+1}+\alpha^{K+2}}\\ &= \frac{1-\alpha-\alpha^{K+1}+\alpha^{K+2}K\left(1-\alpha^{-1}\right)}{1-\alpha-\alpha^{K+1}+\alpha^{K+2}}\\ &\overset{(b)}{<} 1. \end{aligned} \quad (29)$$

Here, (b) is satisfied by conditions of $K > 1$ and $1-\alpha^{-1} = 1-(\beta_0+1) < 0$.

APPENDIX B

Proof of Lemma 1. Firstly, give a function of x

$$w(x,k,j) = \frac{H^2+(x)^2}{H^2+(x+jd)^2}, \quad (30)$$

where x represents $x_k, j = i-k$. Thus, (19) can be turned into

$$\Gamma(x,k) = \sum_{j=1}^{K-k} P_{j+k} w(x,k,j) + \frac{\sigma_N^2\cdot\left(H^2+x^2\right)}{\mathcal{A}}. \quad (31)$$

Then, the first-order derivative and the second-order derivative of (30) achieved as

$$w'(x,k,j) = \frac{2jd(x^2+xjd-H^2)}{(H^2+(x+jd)^2)^2}, \quad (32)$$

and

$$w''(x,k,j) = 2jd\frac{\Psi(x)-\Phi(x)}{(H^2+(x+jd)^2)^3}, \quad (33)$$

respectively. Here, $j = 1\cdots K-k$, $\Phi(x) = 2x^3+3jdx^2$, and $\Psi(x) = 6H^2x+5jdH^2+(jd)^3$. Therefore, the first-order derivative and the second-order derivative of (31) can be expressed as

$$\Gamma'(x,k) = \sum_{j=1}^{K-k} P_{j+k} w'(x,k,j) + \frac{2\sigma_N^2 x}{\mathcal{A}}. \quad (34)$$

and

$$\Gamma''(x,k) = \sum_{j=1}^{K-k} P_{i+k} w''(x,k,j) + \frac{2\sigma_N^2}{\mathcal{A}} \quad (35)$$

respectively. At last, we analyze the function of (32), (33), (34), (35). Obviously, for $x \geq \sqrt{\left(\frac{d}{2}\right)^2 + H^2} - \frac{d}{2}$, we have $w'(x,k,j) \geq 0$, $0 \leq k \leq K$. Based on (34), we further get $\Gamma'(x,k) > 0$. So, $w(x,k,j)$ and $\Gamma(x,k)$ are monotonically increasing function with $x \geq \sqrt{\left(\frac{d}{2}\right)^2 + H^2} - \frac{d}{2}$. For the case of $x < \sqrt{\left(\frac{d}{2}\right)^2 + H^2} - \frac{d}{2}$, we firstly get $w''(x,k,j) > 0$, $0 \leq k \leq K$. Based on (35), we have $\Gamma''(x,k) > 0$. Thus, $w(x,k,j)$ and $\Gamma(x,k)$ are lower concave function with $x < \sqrt{\left(\frac{d}{2}\right)^2 + H^2} - \frac{d}{2}$. Lemma 1 is proved.

APPENDIX C

We just need to prove that the IpN of all the vehicles in $\boldsymbol{V}_0^{k'-1}$ is not increase during the platoon adjusting, as the unchanged transmission power. Firstly, note the horizontal distance and the channel gain between the UAV and V_k as $x'_k = \gamma \cdot x_k$ and g'_k respectively for the period of platoon adjusting. Following from $x_k - x'_k \leq d$ (because only one vehicle leaving for one time), we get the range of γ

$$1 \geqslant \gamma \geqslant 1 - \frac{d}{x_k}. \tag{36}$$

Then, we calculate the IpN at different moments. The IpN at the beginning of platoon adjusting ($x'_k = x_k$) is

$$\begin{aligned} I'_k &= \sum_{i \in \boldsymbol{V}_{k+1}^{k'-1}} P_i g_i + \sum_{i \in \boldsymbol{V}_{k'+1}^{K}} P_i g_i + \sigma_N^2 \\ &= I_k - P_{k'} g_{k'}, \end{aligned} \tag{37}$$

and the IpN during the platoon adjusting is

$$I''_k = \sum_{i \in \boldsymbol{V}_{k+1}^{k'-1}} P_i g_i + \sum_{i \in \boldsymbol{V}_{k'+1}^{K}} P_i g'_i + \sigma_N^2 \tag{38}$$

where $g'_i = \frac{A}{H^2 + (x'_i)^2}$.
Thus, the variation of I_k is expressed as

$$\begin{aligned} \Delta_I &= I_k - I''_k \\ &= \sum_{i \in \boldsymbol{V}_{k'+1}^{K}} P_i g_i + P_k g_k - \sum_{i \in \boldsymbol{V}_{k'+1}^{K}} P_i g'_i \\ &= \sum_{i \in \boldsymbol{V}_{k'+1}^{K}} P_i g_i + \beta_k \left(\sum_{i \in \boldsymbol{V}_{k'+1}^{K}} P_i g_i + \sigma_N^2 \right) \\ &\quad - \sum_{i \in \boldsymbol{V}_{k'+1}^{K}} P_i g'_i \\ &> \sum_{i \in \boldsymbol{V}_{k'+1}^{K}} P_i \left[(1+\beta_k) g_i - g'_i \right] \\ &\approx \mathcal{A} \sum_{i \in \boldsymbol{V}_{k'+1}^{K}} P_i \left[(1+\beta_k) \frac{1}{H^2 + (x_i)^2} - \frac{1}{H^2 + (x'_i)^2} \right]. \end{aligned} \tag{39}$$

Suppose $\left[(1+\beta_k) \frac{1}{H^2+(x_i)^2} - \frac{1}{H^2+(x'_i)^2} \right] < 0$, and set $\beta_k \geq 1$, we get:

$$\begin{aligned} & (1+\beta_k) \frac{1}{H^2 + (x_i)^2} - \frac{1}{H^2 + (x'_i)^2} < 0 \\ & \Rightarrow (1+\beta_k) \frac{1}{H^2 + (x_i)^2} < \frac{1}{H^2 + (x'_i)^2} \\ & \Rightarrow (1+\beta_k) H^2 + (1+\beta_k) (x'_i)^2 < H^2 + (x_i)^2 \\ & \Rightarrow \beta_k H^2 < (x_i)^2 \left[1 - (1+\beta_k) \gamma^2 \right] \\ & \Rightarrow 1 - (1+\beta_k) \gamma^2 > \frac{\beta_k H^2}{(x_i)^2} \\ & \Rightarrow \gamma^2 < \frac{1}{1+\beta_k} \left(1 - \frac{\beta_k H^2}{(x_i)^2} \right). \end{aligned} \tag{40}$$

From $H > d$, above result goes to

$$\begin{aligned} \gamma^2 &< \frac{1}{1+\beta_k} \left(1 - \frac{\beta_k H^2}{(x_i)^2} \right) \\ &< \frac{1}{1+\beta_k} \left(1 - \frac{d^2}{(x_i)^2} \right) \\ &< \left(1 - \frac{d}{x_k} \right)^2. \end{aligned} \tag{41}$$

(41) is contradictory to (36), thus we get

$$\left[(1+\beta_k) \frac{1}{H^2 + (x_i)^2} - \frac{1}{H^2 + (x'_i)^2} \right] \geq 0. \tag{42}$$

Easy to get $\Delta_I = I_k - I''_k \geq 0$, and $I_k \geq I''_k$. Thus, the SINR of V_k after platoon adjusting is

$$\beta''_k = \frac{P_k^r}{I''_k} \geq \frac{P_k^r}{I_k} = \beta_k. \tag{43}$$

APPENDIX D

Proof of Lemma 2. According to Algorithm 3, for $V_j \in \boldsymbol{V}_{k'+1}^{V_l}$, the transmission power:

$$P'_j = P_{j-1}. \tag{44}$$

Following from (44), the received power at UAV is expressed as

$$\begin{aligned} P'_j g'_j &= P_{j-1} g'_j \\ &\overset{(a)}{\leq} P_{j-1} g_{j-1} \\ &= P_{j-1} g_{j-1}. \end{aligned} \tag{45}$$

where (a) is satisfied by that fact that the channel gain of vehicles decreases from PL to the last PM.

The sum received power at UAV for vehicles behind the leaving vehicle:

$$\begin{aligned} \sum_{j \in \boldsymbol{V}_{k'+1}^{K}} P'_j g'_j &= \sum_{j \in \boldsymbol{V}_{k'+1}^{K-1}} P'_j g'_j + P_K g'_K \\ &< \sum_{j \in \boldsymbol{V}_{k'+1}^{K-1}} P_{j-1} g_{j-1} + P_K g_K \end{aligned}$$

$$= \sum_{j \in \boldsymbol{V}_{k'}^{K-2}} P_j g_j + P_K g_K$$
$$< \sum_{j \in \boldsymbol{V}_{k'}^{K}} P_j g_j. \tag{46}$$

APPENDIX E

During the platoon changing period, the channel states between the UAV and platoon vehicles are time-varying. From Section V-A and Section V-C, we know that the power needs to change with the channel states, or the SINR of vehicles will drop below the preset value. However, adjusting the power in real-time brings a high control cost for the system. In this paper, we consider that every vehicle changes power no more than one time for the platoon adjusting. What's more, the adjusting should be executed at the beginning of platoon changing, according to Section V-A.

From Section V-B2, the vehicles that belong to $\boldsymbol{V}_{k'+1}^{K}$ (whose SINR equal to β_0 at the beginning) should not decrease their power to avoid the SINRs below β_0. Meanwhile, the best choice for vehicles with undiminished SINR is fixing their power, otherwise, the vehicles have to increase the power to ensure their SINR is not lower than β_0. Thus, we always have $P'_k \geq P_k$ and $\beta'_k \geq \beta_0$, where P'_k and β'_k are the transmission power and SINR of vehicle k during the platoon changing.

We get $\beta'_k \geq \min\{\beta_k(x_b), \beta_k(x_e)\} \geq \beta_0$ with $\beta_k(x_b) \geq \beta_0$ and $\beta_k(x_e) \geq \beta_0$, according to Theorem 3. Here, $x_b = kd$, $x_e = (k-1)d$, $1 \leq k \leq K$. Therefore, to minimize the transmission power, we suppose $\beta_k(x_b) = \beta_k(x_e) = \beta_0$. The corresponding transmission power $P_k(x_b)$ and $P_k(x_e)$ are expressed as below:

$$\begin{aligned} P_k(x_b) &= (\beta_0 + 1)\frac{g_{k+1}}{g_k} P'_{k+1} \\ &= \lambda_{k+1} P'_{k+1} \geq P_k = \frac{P_{k-1}}{\lambda_k}, \end{aligned} \tag{47}$$

$$\begin{aligned} P_k(x_e) &= (\beta_0 + 1)\frac{g_k}{g_{k-1}} P'_{k+1} = \lambda_k P'_{k+1} \\ &= \frac{P_{k-1}}{P_k} P'_{k+1} \geq \frac{P_{k-1}}{\lambda_{k+1}}. \end{aligned} \tag{48}$$

Thus, $P'_k \geq \max\left\{\frac{P_{k-1}}{\lambda_k}, \frac{P_{k-1}}{\lambda_{k+1}}\right\}$. To guarantee the SINR of vehicles in $\boldsymbol{V}_0^{k'-1}$, we have $P'_k \leq P_{k-1}$. In summary, $\max\left\{\frac{P_{k-1}}{\lambda_k}, \frac{P_{k-1}}{\lambda_{k+1}}\right\} < P'_k \leq P_{k-1}$.

ACKNOWLEDGMENT

The authors would like to sincerely thank Prof. Bo Yang, Department of Automation, Shanghai Jiao Tong University, and Fan Yang, School of Informatics, Xiamen University, for their help to analyze the simulation results.

REFERENCES

[1] H. G. Moussa and W. Zhuang, "Energy- and delay-aware two-hop NOMA-enabled massive cellular IoT communications," *IEEE Internet Things J.*, vol. 7, no. 1, pp. 558–569, Jan. 2020.

[2] Z. Ding, R. Schober, P. Fan, and H. V. Poor, "Simple semi-grant-free transmission strategies assisted by non-orthogonal multiple access," *IEEE Trans. Commun.*, vol. 67, no. 6, pp. 4464–4478, Jun. 2019.

[3] X. Diao, J. Zheng, Y. Wu, and Y. Cai, "Joint computing resource, power, and channel allocations for D2D-assisted and NOMA-based mobile edge computing," *IEEE Access*, vol. 7, pp. 9243–9257, 2019.

[4] Z. Ding, J. Xu, O. A. Dobre, and H. V. Poor, "Joint power and time allocation for NOMA–MEC offloading," *IEEE Trans. Veh. Technol.*, vol. 68, no. 6, pp. 6207–6211, Jun. 2019.

[5] Z. Wang, C. Wen, Z. Fan, and X. Wan, "A novel price-based power allocation algorithm in non-orthogonal multiple access networks," *IEEE Wireless Commun. Lett.*, vol. 7, no. 2, pp. 230–233, Apr. 2018.

[6] J. Zhang, X. Tao, H. Wu, N. Zhang, and X. Zhang, "Deep reinforcement learning for throughput improvement of the uplink grant-free NOMA system," *IEEE Internet Things J.*, vol. 7, no. 7, pp. 6369–6379, Jul. 2020.

[7] X. Shen, J. Gao, W. Wu, K. Lyu, M. Li, W. Zhuang, X. Li, and J. Rao, "AI-assisted network-slicing based next-generation wireless networks," *IEEE Open J. Veh. Technol.*, vol. 1, pp. 45–66, 2020.

[8] W. Wu, N. Chen, C. Zhou, M. Li, X. Shen, W. Zhuang, and X. Li, "Dynamic RAN slicing for service-oriented vehicular networks via constrained learning," *IEEE J. Sel. Areas Commun.*, vol. 39, no. 7, pp. 2076–2089, Jul. 2021.

[9] L. Xiao, Y. Li, C. Dai, H. Dai, and H. V. Poor, "Reinforcement learning-based NOMA power allocation in the presence of smart jamming," *IEEE Trans. Veh. Technol.*, vol. 67, no. 4, pp. 3377–3389, Apr. 2018.

[10] Y. Chen, L. Wang, Y. Ai, B. Jiao, and L. Hanzo, "NOMA in vehicular communications," in *Multiple Access Techniques for 5G Wireless Networks and Beyond*. Springer, 2019, pp. 333–366.

[11] B. Di, L. Song, Y. Li, and Z. Han, "V2X meets NOMA: Non-orthogonal multiple access for 5G-enabled vehicular networks," *IEEE Wireless Commun.*, vol. 24, no. 6, pp. 14–21, Dec. 2017.

[12] J. Kim, Y. Han, and I. Kim, "Efficient groupcast schemes for vehicle platooning in V2V network," *IEEE Access*, vol. 7, pp. 171333–171345, 2019.

[13] W. U. Khan, F. Jameel, G. A. S. Sidhu, M. Ahmed, X. Li, and R. Jäntti, "Multiobjective optimization of uplink NOMA-enabled vehicle-to-infrastructure communication," *IEEE Access*, vol. 8, pp. 84467–84478, 2020.

[14] R. Wang, J. Wu, and J. Yan, "Resource allocation for D2D-enabled communications in vehicle platooning," *IEEE Access*, vol. 6, pp. 50526–50537, 2018.

[15] S. Gurugopinath, P. C. Sofotasios, Y. Al-Hammadi, and S. Muhaidat, "Cache-aided non-orthogonal multiple access for 5G-enabled vehicular networks," *IEEE Trans. Veh. Technol.*, vol. 68, no. 9, pp. 8359–8371, Sep. 2019.

[16] S. Kuk, Y. Park, and H. Kim, "Pseudo-broadcast: An alternative mode of vehicular communication for platooning," *IEEE Commun. Mag.*, vol. 57, no. 6, pp. 56–61, Jun. 2019.

[17] P. Wang, B. Di, H. Zhang, K. Bian, and L. Song, "Platoon cooperation in cellular V2X networks for 5G and beyond," *IEEE Trans. Wireless Commun.*, vol. 18, no. 8, pp. 3919–3932, Aug. 2019.

[18] M. Boban, T. T. V. Vinhoza, M. Ferreira, J. Barros, and O. K. Tonguz, "Impact of vehicles as obstacles in vehicular ad hoc networks," *IEEE J. Sel. Areas Commun.*, vol. 29, no. 1, pp. 15–28, Jan. 2011.

[19] N. Cheng, F. Lyu, W. Quan, C. Zhou, H. He, W. Shi, and X. Shen, "Space/aerial-assisted computing offloading for IoT applications: A learning-based approach," *IEEE J. Sel. Areas Commun.*, vol. 37, no. 5, pp. 1117–1129, May 2019.

[20] H. Wu, J. Chen, W. Xu, N. Cheng, W. Shi, L. Wang, and X. Shen, "Delay-minimized edge caching in heterogeneous vehicular networks: A matching-based approach," *IEEE Trans. Wireless Commun.*, vol. 19, no. 10, pp. 6409–6424, Oct. 2020.

[21] R. Molina-Masegosa, M. Sepulcre, J. Gozalvez, F. Berens, and V. Martinez, "Empirical models for the realistic generation of cooperative awareness messages in vehicular networks," *IEEE Trans. Veh. Technol.*, vol. 69, no. 5, pp. 5713–5717, May 2020.

[22] J. Lunze, "Design of the communication structure of cooperative adaptive cruise controllers," *IEEE Trans. Intell. Transp. Syst.*, vol. 21, no. 10, pp. 4378–4387, Oct. 2020.

[23] S. Chen, J. Hu, Y. Shi, L. Zhao, and W. Li, "A vision of C-V2X: Technologies, field testing, and challenges with Chinese development," *IEEE Internet Things J.*, vol. 7, no. 5, pp. 3872–3881, May 2020.

[24] A. Bazzi, A. Zanella, and B. M. Masini, "Optimizing the resource allocation of periodic messages with different sizes in LTE-V2V," *IEEE Access*, vol. 7, pp. 43820–43830, 2019.
[25] Y. Sun, L. Xu, Y. Tang, and W. Zhuang, "Traffic offloading for online video service in vehicular networks: A cooperative approach," *IEEE Trans. Veh. Technol.*, vol. 67, no. 8, pp. 7630–7642, Aug. 2018.
[26] W. Shi, J. Li, H. Wu, C. Zhou, N. Cheng, and X. Shen, "Drone-cell trajectory planning and resource allocation for highly mobile networks: A hierarchical DRL approach," *IEEE Internet Things J.*, vol. 8, no. 12, pp. 9800–9813, Jun. 2021.
[27] M. Aldababsa, M. Toka, S. Gökçeli, G. K. Kurt, and O. Kucur, "A tutorial on nonorthogonal multiple access for 5G and beyond," *Wireless Commun. Mobile Comput.*, vol. 2018, pp. 1–24, Jun. 2018.
[28] S. Xu, C. Guo, and Z. Li, "NOMA enabled resource allocation for vehicle platoon-based vehicular networks," in *Proc. IEEE GC Wkshps*, Dec. 2019, pp. 1–6.
[29] B. Wang, L. Dai, Y. Zhang, T. Mir, and J. Li, "Dynamic compressive sensing-based multi-user detection for uplink grant-free NOMA," *IEEE Commun. Lett.*, vol. 20, no. 11, pp. 2320–2323, Nov. 2016.
[30] M. Shirvanimoghaddam, M. Condoluci, M. Dohler, and S. J. Johnson, "On the fundamental limits of random non-orthogonal multiple access in cellular massive IoT," *IEEE J. Sel. Areas Commun.*, vol. 35, no. 10, pp. 2238–2252, Oct. 2017.
[31] C. Zhang, Z. Qin, Y. Liu, and K. K. Chai, "Semi-grant-free uplink NOMA with contention control: A stochastic geometry model," in *Proc. IEEE ICC Workshops*, Jun. 2020, pp. 1–6.
[32] Y. Saito, A. Benjebbour, Y. Kishiyama, and T. Nakamura, "System-level performance evaluation of downlink non-orthogonal multiple access (NOMA)," in *Proc. IEEE 24th PIMRC*, Sep. 2013, pp. 611–615.
[33] B. Di, L. Song, and Y. Li, "Sub-channel assignment, power allocation, and user scheduling for non-orthogonal multiple access networks," *IEEE Trans. Wireless Commun.*, vol. 15, no. 11, pp. 7686–7698, Nov. 2016.
[34] Y. Sun, D. W. K. Ng, Z. Ding, and R. Schober, "Optimal joint power and subcarrier allocation for full-duplex multicarrier non-orthogonal multiple access systems," *IEEE Trans. Commun.*, vol. 65, no. 3, pp. 1077–1091, Mar. 2017.
[35] Q. Wu, W. Chen, D. W. K. Ng, and R. Schober, "Spectral and energy-efficient wireless powered IoT networks: NOMA or TDMA?" *IEEE Trans. Veh. Technol.*, vol. 67, no. 7, pp. 6663–6667, Jul. 2018.
[36] Z. Song, Q. Ni, and X. Sun, "Spectrum and energy efficient resource allocation with QoS requirements for hybrid MC-NOMA 5G systems," *IEEE Access*, vol. 6, pp. 37055–37069, 2018.
[37] Y. Zhang, H.-M. Wang, T.-X. Zheng, and Q. Yang, "Energy-efficient transmission design in non-orthogonal multiple access," *IEEE Trans. Veh. Technol.*, vol. 66, no. 3, pp. 2852–2857, Mar. 2017.
[38] Z. Ding, Z. Yang, P. Fan, and H. V. Poor, "On the performance of non-orthogonal multiple access in 5G systems with randomly deployed users," *IEEE Signal Process. Lett.*, vol. 21, no. 12, pp. 1501–1505, Dec. 2014.
[39] J. Harri, F. Filali, and C. Bonnet, "Mobility models for vehicular ad hoc networks: A survey and taxonomy," *IEEE Commun. Surveys Tuts.*, vol. 11, no. 4, pp. 19–41, 4th Quart., 2009.
[40] R. Duan, J. Wang, C. Jiang, H. Yao, Y. Ren, and Y. Qian, "Resource allocation for multi-UAV aided IoT NOMA uplink transmission systems," *IEEE Internet Things J.*, vol. 6, no. 4, pp. 7025–7037, Aug. 2019.

YANGLONG SUN (Graduate Student Member, IEEE) received the B.S. and M.S. degrees from Zhengzhou University, China, in 2011 and 2014, respectively. He is currently pursuing the Ph.D. degree in communication engineering with Xiamen University, China. He was a Visiting Ph.D. Student at the Broadband Communications Research (BBCR) Laboratory, Department of Electrical and Computer Engineering, University of Waterloo, Waterloo, ON, Canada, from 2018 to 2019. His research interests include vehicular ad hoc networks, resource allocation in IoV, mobile 5G networks, and intelligent transportation systems.

KE ZHENG received the B.E. degree from the Changsha University of Science and Technology, Changsha, China, in 2019. She is currently pursuing the M.S. degree with the Department of Information and Communication Engineering, Xiamen University, Xiamen, China. Her research interests include vehicle networking communications, NOMA, and 5G networks.

YULIANG TANG (Member, IEEE) received the M.S. degree from the Beijing University of Posts and Telecommunications, China, in 1996, and the Ph.D. degree in information and communication engineering from Xiamen University, in 2009. He is currently a Professor with the Department of Information and Communication Engineering, Xiamen University. He has published more than 90 papers in journals and international conferences. He has been granted over 20 patents in his research areas. His research interests include wireless communication, 5G and beyond, and vehicular ad hoc networks.